

# Automated design and implementation of a NOR gate in *Pseudomonas putida*

Huseyin Tas<sup>1</sup>, Lewis Grozinger<sup>2</sup>, Angel Goñi-Moreno<sup>2,3,\*</sup>, and Victor de Lorenzo<sup>1,\*</sup>

<sup>1</sup>Systems Biology Department, Centro Nacional de Biotecnología-CSIC, Madrid, Spain

<sup>2</sup>School of Computing, Newcastle University, Newcastle Upon Tyne, UK

<sup>3</sup>Centro de Biotecnología y Genómica de Plantas, Universidad Politécnica de Madrid, Instituto Nacional de Investigación y Tecnología Agraria y Alimentaria, Madrid, Spain

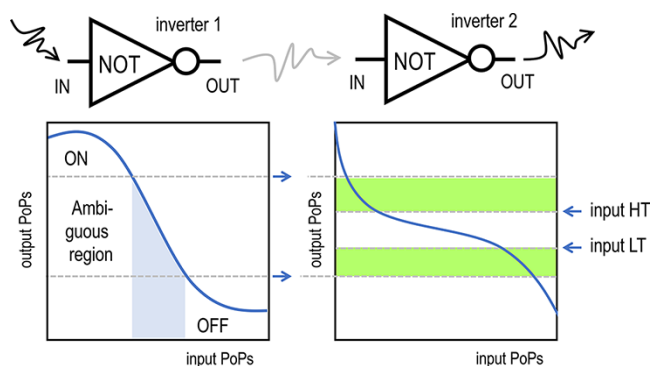
\*Corresponding authors: E-mails: [vdlorenzo@cnb.csic.es](mailto:vdlorenzo@cnb.csic.es) and [angel.goni@upm.es](mailto:angel.goni@upm.es)

## Abstract

Boolean NOR gates have been widely implemented in *Escherichia coli* as transcriptional regulatory devices for building complex genetic circuits. Yet, their portability to other bacterial hosts/chassis is generally hampered by frequent changes in the parameters of the INPUT/OUTPUT response functions brought about by new genetic and biochemical contexts. Here, we have used the circuit design tool CELLO for assembling a NOR gate in the soil bacterium and the metabolic engineering platform *Pseudomonas putida* with components tailored for *E. coli*. To this end, we capitalized on the functional parameters of 20 genetic inverters for each host and the resulting compatibility between NOT pairs. Moreover, we added to the gate library three inducible promoters that are specific to *P. putida*, thus expanding cross-platform assembly options. While the number of potential connectable inverters decreased drastically when moving the library from *E. coli* to *P. putida*, the CELLO software was still able to find an effective NOR gate in the new chassis. The automated generation of the corresponding DNA sequence and *in vivo* experimental verification accredited that some genetic modules initially optimized for *E. coli* can indeed be reused to deliver NOR logic in *P. putida* as well. Furthermore, the results highlight the value of creating host-specific collections of well-characterized regulatory inverters for the quick assembly of genetic circuits to meet complex specifications.

**Key words:** logic gates; *Pseudomonas putida*; inverter; computer-assisted design; genetic circuit

## Graphical Abstract



## 1. Introduction

NOR logic gates (Figure 1A) are useful digital devices due to their functional completeness, i.e. any other logic function can be built by combining NOR gates. Therefore, they are the basis of many

of the complex digital networks that rule the functioning of electronic devices and control systems (1). It is thus not surprising that recent efforts to develop operational systems for engineering signal processing in bacteria have also attempted the implemen-

Submitted: 13 May 2021; Received (in revised form): 13 July 2021; Accepted: 11 August 2021

© The Author(s) 2021. Published by Oxford University Press.

This is an Open Access article distributed under the terms of the Creative Commons Attribution-NonCommercial-NoDerivs licence (<http://creativecommons.org/licenses/by-nc-nd/4.0/>), which permits non-commercial reproduction and distribution of the work, in any medium, provided the original work is not altered or transformed in any way, and that the work is properly cited. For commercial re-use, please contact [journals.permissions@oup.com](mailto:journals.permissions@oup.com)

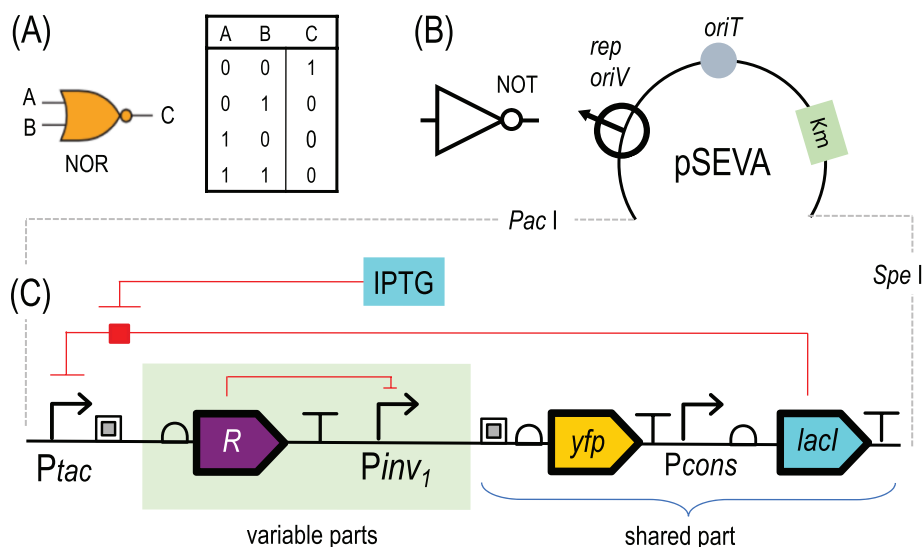


**Figure 1.** NOR function and NOT logic implementation. Overview of NOR gates and constructs built for measurements. (A) Schematics of a NOR gate and its truth table. (B) Regulatory inverter backbone in SEVA format. Each gate and sensory module shares the same standardized vector frame. (C) Genetic devices and the structure of the functional part. The devices share a part containing the *yfp* cassette and *Ptac/lacI* expression system inducible with IPTG.

tation of NOR gates with available regulatory parts (2, 3). The NOR function gets two inputs and delivers one output, which is '1' if none of the inputs is present and '0' in any other case. The use of transcriptional repressors to implement logic inverter functions (i.e. NOT) along regulatory cascades, where each regulator controls the performance of the next (4), is key to implement such gates. Yet, unlike electronic parts, regulated promoters are not digital but their response functions are subject to different parameters and kinetic ranges, often dependent on context and environmental conditions (5). This makes the connection of compatible parts for building more complex devices far from easy. NOT gates must be compatible to secure that the output of a gate matches the input of the next; this guarantees that the signal can be processed along a regulatory cascade. This challenge was addressed and solved to a large extent in 2016 with the CELLO software for genetic circuit design automation (3). The same tool was subsequently optimized for other organisms (6), including yeast (7). More recently, the CELLO-based genetic circuitry has been shown to be capable of adaptive cellular computations that can respond to the alterations in the environment and be tuned dynamically (8). The CELLO platform is based on the thorough experimental characterization and parameterization of a collection of 20 naturally occurring and optimized genetic inverters in *Escherichia coli*, i.e. a series of promoters and cognate repressors. Transcriptional isolation implemented for promoter units via ribozymes and the choice of strong terminators for the gates to eliminate intra-circuitry transcriptional read-throughs, together with observed toxicity levels of gates, are key angles of the platform. Processing of the rich dataset thereby empowered computational predictions of compatible and incompatible gates. This in turn enabled the automatic design of two or more signal-processing control layers in the same cell and the ability to implement virtually any given function. The practical angle of this approach is that the CELLO algorithms build a circuit diagram, look for connectable gates and simulate its performance. Finally, the system translates the desired logic circuit into a specific DNA sequence that can be synthesized and experimentally tested (3).

Despite some shortcomings, CELLO has enabled the construction of genetic circuits of unprecedented complexity and rationally designed performance (9, 10). One question is whether the same gates and their associated parameters—that facilitate automated circuit design in *E. coli*—can be directly reused in other hosts and chassis, in particular in platforms of interest for industrial and environmental synthetic biology. One of such platforms is the Gram-negative soil bacterium *Pseudomonas putida*, one strain of which (the *P. putida* KT2440) has emerged as a chassis of choice for a suite of biotechnological applications (11–13). *P. putida* KT2440 is naturally pre-evolved not only with a remarkable metabolic flexibility but also with an outstanding tolerance to many of the typical physicochemical stresses that frame industrial processes (11, 14, 15). In a first attempt to capitalize on the CELLO platform in this strain, the 20 NOT gates available for *E. coli* were recreated in standardized low-copy number vectors (16). The INPUT (isopropyl thiogalactopyranoside, IPTG)/OUTPUT (yellow fluorescence protein, YFP) response functions of each separate construct were then determined in *P. putida* and the results between the two hosts compared (16). Not surprisingly, most gates behaved very differently in each biological recipient, both qualitatively and quantitatively. The outcome of such an exercise puts numbers to the question about the portability of genetic devices, not just between *E. coli* and *P. putida* but among species. Is thus reusability of genetic devices (even of their simplest building blocks) between hosts impossible? In this work, we have addressed this question by exploring the portability of the inverters formerly developed as part of the CELLO platform of *E. coli* for building an effective NOR gate in *P. putida*. To this end, we built on the formalisms for scoring gate compatibility developed by (3) and (5). These are based on the fact that the interplay between host's genetic and biochemical context do change expression levels of a given gate, its dynamic range and even its logic function. In order to tackle this issue, the upper and lower input/output thresholds of all inverters available in a library were scored in the host of interest. Such metrics enabled the identification of combinations that can then be converted by the CELLO system in composed gates and materialized as specific

DNA sequences. We show below the efficacy of this approach for the automated design of a functional NOR gate in *P. putida*. Moreover, the data below will assist in implementing CELLO or CELLO-like approaches in hosts other than *E. coli*.

## 2. Materials and methods

### 2.1 Host strain, inverter library and devices for upstream inputs

Reference strain *P. putida* KT2440 is described in detail in (14, 17). A compilation of constructs bearing a suite of promoter/repressor pairs borne by broad host range plasmids can be found in (16). The subset of such a collection used in this work corresponds to those bearing the genetic inverters separately cloned in low-copy number vectors pSEVA221 as well as three additional plasmids of reference for quantifying autofluorescence and promoter activity (3, 16). In addition, three plasmids encoding promoters inducible in *P. putida* were added to the collection as devices for parameterization of the upstream inputs available for gate and circuit design in this bacterium (Supplementary Figure S1). Plasmids were constructed based on pAN1718 (*Ptac/LacI*), pAN1719 (*Ptet/TetR*) and pAN1720 (*PBAD/AraC*) sensor measurement plasmids (3). Forward (5'-cctagattaataaaacacccctgtattactgtttatgtaagc-3') and reverse (5'-gtctaaactagt cgtccggcgtagaggatc-3') primers were used to amplify the sensory parts of above-mentioned plasmids along with the introduction of *PacI* and *SpeI* restriction sites. PCR products were then digested and cloned into pSEVA221 in *PacI* and *SpeI* sites yielding pSEVA221::1718, pSEVA221::1719 and pSEVA221::1720 sensor measurement plasmids. The complete list of DNA constructs used in this study is compiled in Supplementary Table S1. Their DNA sequences can be found in the plasmid sequence files of the Supplementary Information. All constructs are available through the Standard European Vector Architecture (SEVA) repository of the CNB-CSIC (<http://seva-plasmids.com/>).

### 2.2 Design of a NOR gate with CELLO software

For designing a NOR gate with the CELLOCAD software, a user constraints file (UCF) specific for *P. putida* was uploaded to <http://cellocad.org> (CAD files in Supplementary Information). The format of this file (*PseudomonasputidaKT2440.UCF.json*) was kept the same as the one that CELLO has for *E. coli* (*Eco1C1G1T1.UCF.json*). The gate response functions were updated based on experimental results generated for each inverter and reference promoter in *P. putida*. In order for the software to automatically generate DNA designs of effective NOR gates, we entered through a Verilog interface the sequences of the characterized promoters. The program was then run and the platform returned the output files as a package (CAD files in Supplementary Information) that includes the simulation values, the circuit and output plasmid maps and all related data to CELLO's calculations. In this study, we merged the circuit and output plasmids in a single broad host range SEVA format plasmid. In addition, we cloned the synthetic DNA sequences in plasmid vectors with low (pSEVA221) and medium (pSEVA231) copy numbers in *P. putida* via cloning at *PacI* and *SpeI* restriction enzyme recognition sites. The synthesized sequence can be found in Supplementary Information as a GenBank file.

### 2.3 Culture conditions

Growth of *P. putida* KT2440 strain transformed with plasmids bearing the genetic inverters, the constructs of reference and the DNA encoding the automatically designed NOR gate were handled as

explained in (16) and (5). In brief, cultures of each of the transformants under examination were grown overnight in M9 minimal medium with citrate as the sole carbon source for synchronizing the cells' growth states. These were then diluted ~600-fold for the inoculation of 96-well plates filled with 200  $\mu$ l of the same medium and inducers to the following concentrations: 1 mM IPTG for *Ptac/LacI*, 100 ng/ml anhydrotetracycline (aTc) for *Ptet/TetR* and 20 mM arabinose for *PBAD/AraC*. Plates were then grown at 30°C to late exponential stage, transferred to a cold platform at 4°C for stopping growth and the samples taken for fluorescence cytometry analyses as described in (16).

## 3. Results and discussion

The starting point of this work is the collection of 20 genetic inverters (derived from 12 unique repressors with several ribosomal binding sequences) shaped by transcriptional repressors and target promoters, assembled in a broad host range standardized vector frame (16; Figure 1B). This enabled precise determination of the parameters of the INPUT/OUTPUT response function when placed in *P. putida* and their comparison with those reported for *E. coli* in the context of the CELLO platform (16). The rationale for the identification of inverters amenable to combinations in a higher-order logic gate is sketched in Supplementary Figure S2. Given that the dose-response curves of the genetic inverters are not digital, the critical issue is the management of thresholds for interpreting their input and output levels as Boolean signals. In practical terms, thresholds (either higher or lower) are the sectors of the response function of the NOT gates below which the output is not directly amenable to digital logic. Such thresholds divide the continuous-valued input and output ranges into regions. Expression levels that lie in the upper and lower sectors can be operationally interpreted as either digital ON or OFF states, respectively. Yet, these regions are separated by an intermediate set of values (the 'ambiguous region') within which the logic values of inputs and outputs are unclear (Supplementary Figure S2). The purpose of such a region is to clearly separate the ON and OFF states such that intermediate values cannot (within a given confidence level) lead to the misinterpretation of YES or NO signals leading to circuit failure. The optimum size of the ambiguous region, which defines the steepness of the digital-like behavior of the gate thresholding region, is therefore related to the signal-to-background ratio at both ON and OFF expression levels. If the ratio changes when the gate at stake is placed in different hosts (or contexts at large), such thresholds need to be redefined accordingly.

Out of the 362 possible combinations of genetic inverters of the CELLO collection in *E. coli*, 162 of them turn out to be compatible upon the application of a specific set of rules to the experimental data available for this host (3). This high number of compatible gates is not surprising as all the parts that compose the inverters were optimized for *E. coli*. But how do these gates behave in *P. putida*? In order to inspect the portability of the same inverters and their fitting in the new host, each of the genetic devices (Figure 1C) were recloned in broad host range vectors, passed to the new Gram-negative host and their input-output (IPTG-YFP) response functions parameterized experimentally (16). To this end, raw fluorescence cytometry data were converted to relative promoter units (RPU) as indicated in (16). Adoption of such standardized units enabled a faithful assessment of the dynamic range of each negatively regulated promoter. Furthermore, overlaying the resulting data on Hill equations (3, 16) exposed the separate response functions of each genetic device in *P. putida*.

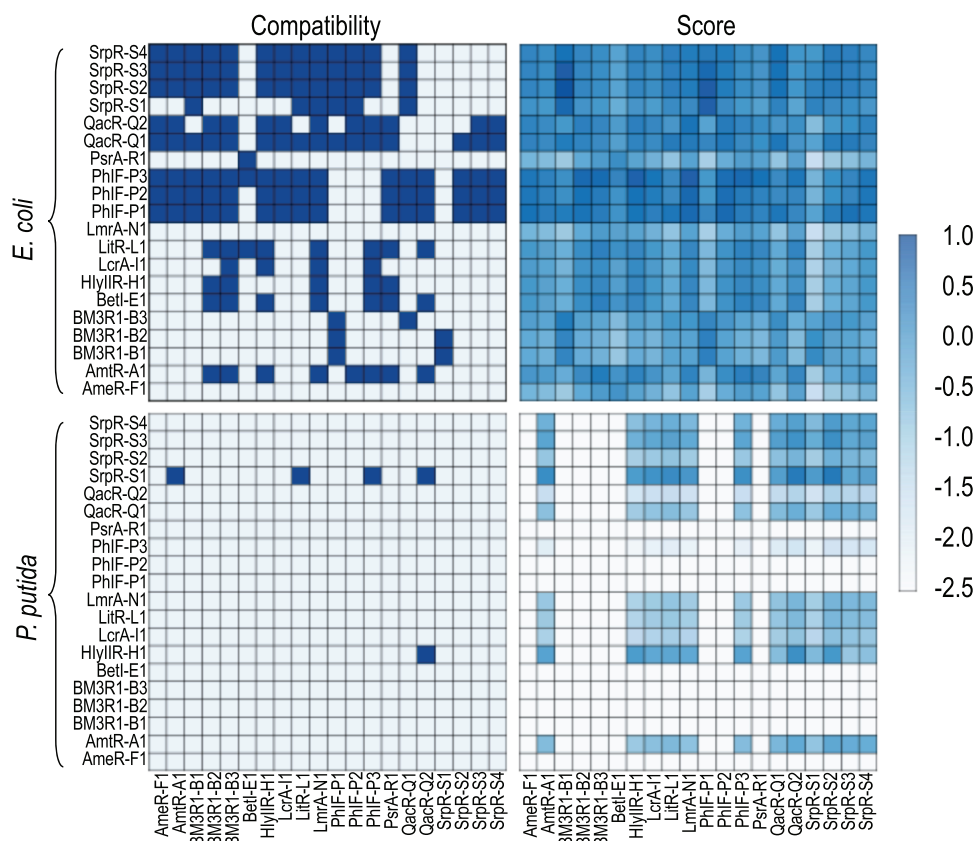


**Figure 2.** Pair compatibility and scoring comparison of 20 genetic inverters in *E. coli* and *P. putida*. The organization of each of the constructs tested is sketched and the parameters described in detail in (3) for *E. coli* and (16) for *P. putida*. Compatibility and scoring matrices given for *E. coli* and *P. putida*, X-axes for input gates and Y-axes for output gates. Binary color code in compatibility matrices shows pair compatibilities (dark blue compatible, light blue incompatible). Number of compatible gates in *E. coli* is much greater than *P. putida* equivalent. Adapted scoring system (5) shows how far gates are from being (in)compatible pairs. Heatmap score  $>0$  indicates compatible and  $<0$  indicates not compatible. Magnitude of color code indicates how (in)compatible they are (note that nonworking inverters are not scored and included as white squares in the scoring graphs for representative purposes).

These analyses immediately qualified the functionality of the individual NOT gates and permitted their pairwise comparison and categorization. With this wealth of data in hand, we set out to determine gate compatibilities. For this, we adopted the scoring system originally developed in (3) and (5), which attempts to identify candidate pairs that are most likely to work when connected *in vivo*. When such restrictive criteria were used to grade gate performance in *P. putida* (Figure 2), only five combinations received the highest compatibility scores (Figure 2, bottom-left). Specifically, the software identified the inverter called SrpR-S1 (3, 5) as the one with the highest compatibility score with several others. While the number of effective gates in *P. putida* was much lower than those identified earlier for *E. coli* (5), it was sufficient for testing *prima facie* the general applicability of the CELLO framework for automated design of composed gates such as NOR in a host other than *E. coli*. To this end, we had to generate additional experimental data on promoters inducible with chemical effectors that could become the inputs of the NOR gate in the new host. For this, we recreated in broad host range vector pSEVA221 the inserts of control plasmids pSEVA221::1718, pSEVA221::1719 and pSEVA221::1720 (Supplementary Figure S1 and Supplementary Table S1) and determined their ON/OFF values as described in (3). Specifically, we measured constructs with *Ptac/LacI*, *Ptet/TetR* and *PBAD/AraC* modules (inducible by IPTG, aTc and arabinose, respectively). Data on these promoters (Supplementary Table S2) increased the number and ranges of transcriptional

outputs and thus expanded the available design space in *P. putida*.

The experimental data on each inverter generated in *P. putida* (16) with low-copy backbone and the results of the characterization of these three promoters thereof were entered in the CelloCAD software (3). The system was then asked to generate a NOR gate and the software returned predictions of viable NOR gates, which were simulated with the CelloCAD tool as well. The one shown in Figure 3 (a combination of the aforementioned SrpR-S1 inverter with the *LacI/Ptac* and *AraC/PBAD*-inducible promoters) was chosen for actual implementation as a DNA segment. The chemically synthesized ~2-kb fragment (CAD files of Supplementary Information) was subsequently cloned in low-copy number pSEVA221 and medium-copy number pSEVA231 vectors (containing constitutively expressed regulator proteins *LacI*, *TetR* and *AraC*), resulting in plasmids pSEVA221::NOR-SrpR\_S1 and pSEVA231::NOR-SrpR\_S1, respectively (plasmid sequence files of Supplementary Information). These were electroporated in *P. putida* KT2440 and the transformants grown and treated with either 1 mM IPTG or 20 mM arabinose, as indicated in the “Materials and Methods” section. The results are shown in Figure 4. Note that despite the limited design space that results from imposing strict compatibility rules, the automated design works well regardless of the copy number of the vector where the synthetic sequence was inserted. The range of values observed experimentally in pSEVA221 (low copy) corresponds more closely to



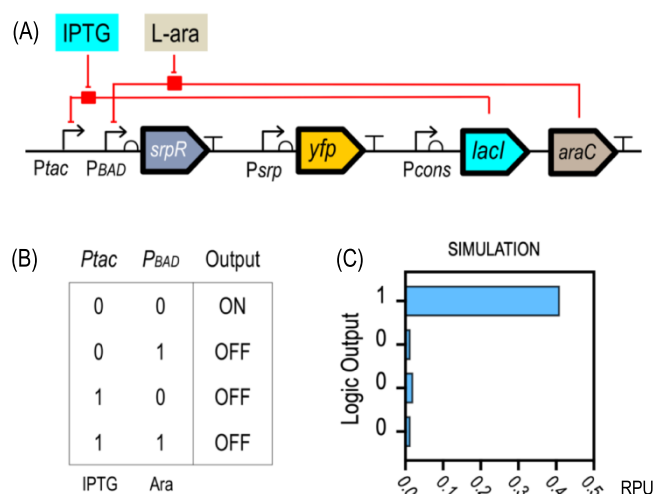


**Figure 3.** Implementation of a NOR gate with DNA parts and sequences delivered by the CELLO software. (A) Schematic representation showing IPTG and L-arabinose inducible circuit. In the implementation of NOR gate, a NOT gate (*SrpR*) is regulated with two inducible systems (*P<sub>tac</sub>*/*LacI* and *P<sub>tet</sub>*/*PBAD*). (B) Truth table for two-input NOR gate system for given inducers. (C) Simulation indicates *in silico* values received from CelloCAD software based on the *P. putida* experimental data inputted. For ON/OFF states of inputs, simulated outputs are shown.

those predicted by the CELLO system. However, in all other respects, the performance of the pSEVA231 constructs is a better fit to the predictions. This is because the greater variance in the RPU measurements of the gate in pSEVA221 reduces the margin of error in the threshold values. Presumably, this difference arises because measurements of cells with higher copy numbers involve the averaging of a greater number of individual fluorescence signals. Higher copy numbers in pSEVA231 measurements may therefore make these measurements less sensitive to fluctuations in individual plasmid copy performance and explained the lower variance observed in pSEVA231 experiments. A sidelight of the construct sketched in Figure 4 (full sequence in the CAD file of Supplementary Information) is that the *PBAD* promoter is placed with no problem downstream of *P<sub>tac</sub>*. Due to the different parameters of the corresponding individual gates in each host, this arrangement is viable and effective in *P. putida* but predicted nonfunctional in *E. coli* due to a roadblocking phenomenon (3). This detail exemplifies how *P. putida*-specific parameters and the intracellular milieu change the design space in a distinct way that is different from that in *E. coli*.

In conclusion, we accredit that the conceptual and technical tools of the CELLO system, initially envisioned for implementation in *E. coli*, can be expanded to other hosts as such, provided that the parameters associated with each inverter result in a reasonable design space for the assembly of genetic devices of growing complexity. In some instances, the behavior of existing gates in a host of choice may suffice for some circuit-building projects, while in others, a suite of host-dedicated inverters and default regulated promoter may need to be constructed. In the case study presented above, a very limited number of gate pairs and RPU ranges were identified as adequate for building a NOR gate, but this may vary in other hosts. An intermediate possibility is adjusting thresholds through a parameter that can be called *threshold multiplier*. This is an arbitrary variable that sets the value of the upper and lower thresholds, thereby determining the size

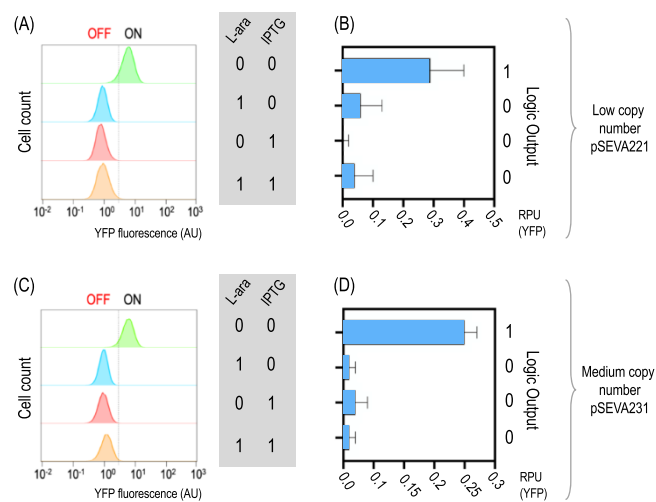


**Figure 4.** Experimental characterization of automatically designed NOR gate in *P. putida*. (A) and (C) are flow cytometer distribution as representative of an actual experiment of NOR gate implementation in *P. putida* for low-copy and medium-copy numbers. For each measure 30k events were collected and auto-gating was applied (covering at least >50% of the events). Results are average of three experimental repeats from three different days. (B) and (D) are YFP values in RPU in low- and medium-copy numbers for 4 combinations of two-input logical operation of the NOR gate. 1 stands for ON and 0 stands for OFF state of the output.

of the ambiguous region for any given NOT gate (Supplementary Figure S2) and thus enabling the expansion of gate compatibility. An analysis of how thresholding might affect the size of the design space in *E. coli* DH5 $\alpha$  and *P. putida* KT2440 is shown in Supplementary Figure S3. A critical consideration is the absolute difference between high and low expression levels. If they are not clearly distant, additional criteria need to be adopted for adjusting the skewness of the ambiguous region to a practical range. To this end, the multiplier can be given separate upper and lower values, thereby enabling asymmetric thresholding. As shown in Supplementary Figure S3, the adoption of asymmetric thresholds expands *in silico* the number of compatible NOT gate pairs in *P. putida* from 5 to 14. We expect these considerations to expand the usefulness of the CELLO platform and facilitate the genetic circuit design in a wider variety of bacteria of industrial and environmental interest. One exciting area of potential application involves the *in situ* bioremediation of chemical pollution, whereby engineered strains should process a number of endogenous and exogenous cues for adapting the expression of biodegradation activities to site-specific circumstances (13, 18).

## Supplementary data

Supplementary data are available at SYNBIOS online.

## Data availability

All data described in this work are freely available upon request at no cost and without restrictions.

## Funding

SETH [RTI2018-095584-B-C42; MINECO/FEDER] and SyCoLiM [ERA-COBIOTECH 2018—PCI2019-111859-2] Projects of the Spanish Ministry of Science and Innovation; the MADONNA [H2020-FET-OPEN-RIA-2017-1-766975]; BioRoboost [H2020-NMBP-

BIO-CSA-2018-820699]; SynBio4Flav [H2020-NMBP-TR-IND/H2020-NMBP-BIO-2018-814650] and MIX-UP [MIX-UP H2020-BIO-CN-2019-870294] Contracts of the European Union; the InGEMIC-SCM [S2017/BMD-3691 FSE, FECER] and BioSinT-CM [Y2020/TCS-6555] Projects of the Comunidad de Madrid. A.G.-M. was also supported by the CONTEXT project from Comunidad de Madrid [Atracción de Talento Program; 2019-T1/BIO-14053] and the Severo Ochoa Program for Centres of Excellence in R&D from the Agencia Estatal de Investigación of Spain [SEV-2016-0672] (2017–2021).

## Acknowledgments

The authors are indebted to Prof. Chris Voigt (MIT) for access to the CELLO platform and Dr Shuyi Zhang (MIT) for help with using the cognate software with *Pseudomonas putida*.

Conflict of interest statement. None declared.

## References

- Huang,Y., Duan,X., Cui,Y., Lauhon,L.J., Kim,K.-H. and Lieber,C.M. (2001) Logic gates and computation from assembled nanowire building blocks. *Science*, **294**, 1313–1317.
- Tamsir,A., Tabor,J.J. and Voigt,C.A. (2011) Robust multicellular computing using genetically encoded NOR gates and chemical ‘wires’. *Nature*, **469**, 212–215.
- Nielsen,A.A., Der,B.S., Shin,J., Vaidyanathan,P., Paralanov,V., Strychalski,E.A., Ross,D., Densmore,D. and Voigt,C.A. (2016) Genetic circuit design automation. *Science*, **352**, aac7341.
- Stanton,B.C., Nielsen,A.A., Tamsir,A., Clancy,K., Peterson,T. and Voigt,C.A. (2014) Genomic mining of prokaryotic repressors for orthogonal logic gates. *Nat. Chem. Biol.*, **10**, 99–105.
- Tas,H., Grozinger,L., Stoof,R., de Lorenzo,V. and Goñi-Moreno,Á. (2021) Contextual dependencies expand the re-usability of genetic inverters. *Nat. Comm.*, **12**, 355.
- Taketani,M., Zhang,J., Zhang,S., Triassi,A.J., Huang,Y.-J., Griffith,L.G. and Voigt,C.A. (2020) Genetic circuit design automation for the gut resident species *Bacteroides thetaiotaomicron*. *Nat. Biotechnol.*, **38**, 962–969.
- Chen,Y., Zhang,S., Young,E.M., Jones,T.S., Densmore,D. and Voigt,C.A. (2020) Genetic circuit design automation for yeast. *Nat. Microbiol.*, **5**, 1349–1360.
- Bartoli,V., Meaker,G.A., di Bernardo,M. and Gorochowski,T.E. (2020) Tunable genetic devices through simultaneous control of transcription and translation. *Nat. Comm.*, **11**, 2095.
- Shin,J., Zhang,S., Der,B.S., Nielsen,A.A. and Voigt,C.A. (2020) Programming *Escherichia coli* to function as a digital display. *Mol. Syst. Biol.*, **16**, e9401.
- Park,Y., Espah Borujeni,A., Gorochowski,T.E., Shin,J. and Voigt,C.A. (2020) Precision design of stable genetic circuits carried in highly-insulated *E. coli* genomic landing pads. *Mol. Syst. Biol.*, **16**, e9584.
- Nikel,P.I. and de Lorenzo,V. (2018) *Pseudomonas putida* as a functional chassis for industrial biocatalysis: from native biochemistry to trans-metabolism. *Metabol. Eng.*, **50**, 142–155.
- Martínez-García,E., Nikel,P.I., Aparicio,T. and de Lorenzo,V. (2014) *Pseudomonas 2.0*: genetic upgrading of *P. putida* KT2440 as an enhanced host for heterologous gene expression. *Microb. Cell Fact.*, **13**, 159.
- Dvořák,P., Nikel,P.I., Damborský,J. and de Lorenzo,V. (2017) Bioremediation 3.0: engineering pollutant-removing bacteria in the times of systemic biology. *Biotechnol. Adv.*, **35**, 845–866.
- Nikel,P.I., Martínez-García,E. and de Lorenzo,V. (2014) Biotechnological domestication of pseudomonads using synthetic biology. *Nat. Rev. Microbiol.*, **12**, 368–379.
- Eng,T., Banerjee,D., Lau,A.K., Bowden,E., Herbert,R.A., Trinh,J., Prah,J.-P., Deutschbauer,A., Tanjore,D. and Mukhopadhyay,A. (2021) Engineering *Pseudomonas putida* for efficient aromatic conversion to bioproduct using high throughput screening in a bioreactor. *Metabol. Eng.*, **66**, 229–238.
- Tas,H., Goñi-Moreno,Á. and Lorenzo,V. (2021) A standardized inverter package borne by broad host range plasmids for genetic circuit design in Gram-negative bacteria. *ACS Synth. Biol.*, **10**, 213–217.
- Belda,E., van Heck,R.G.A., José Lopez-Sanchez,M., Cruveiller,S., Barbe,V., Fraser,C., Klenk,H.-P., Petersen,J., Morgat,A., Nikel,P.I. et al. (2016) The revisited genome of *Pseudomonas putida* KT2440 enlightens its value as a robust metabolic chassis. *Environ. Microbiol.*, **18**, 3403–3424.
- Nikel,P.I. and de Lorenzo,V. (2021) Metabolic engineering for large-scale environmental bioremediation. In: Nielsen J, Stephanopoulos G, Lee SY (eds). *Metabolic Engineering: Concepts and Applications*. Wiley VCH GmbH, Weinheim. pp. 859-890.